Interaction between the diatom Cylindrotheca closterium and a siliceous mortar in a silica-limited environment

Marine Georges, Amel Bourguiba, Mohamed Boutouil, Daniel Chateigner, Orianne Jolly, Pascal Claquin

Interaction between the diatom *Cylindrotheca closterium* and a siliceous mortar in a silica-limited environment

Marine Georges[a], Amel Bourguiba[a], Mohamed Boutouil[a], Daniel Chateigner[b], Orianne Jolly[c], Pascal Claquin[cd]

[a] COMUE NU, Laboratoire de Recherche ESITC Caen, 1 Rue Pierre et Marie Curie, 14610 Epron, France.

marine.georges@esitc-caen.fr; amel.bourguiba@esitc-caen.fr; mohamed.boutouil@esitc-caen.fr

[b]Normandie Université. CRISMAT UMR CNRS n°6508. ENSICAEN. IUT Caen. Université de Caen Normandie. 6 boulevard Maréchal Juin. 14050 Caen. France

daniel.chateigner@ensicaen.fr

[c]Normandie Université. Université de Caen Normandie. F-14032. Caen. France

[d]Laboratoire Biologie des ORganismes et Ecosystèmes Aquatiques (BOREA, UMR 8067), Sorbonne Université, Muséum National d'Histoire Naturelle, CNRS, Université Pierre et Marie Curie, Université de Caen Normandie, IRD 207, Université des Antilles. Centre de Recherches en Environnement Côtier (CREC) - Station Marine, BP49, 54, rue du Docteur Charcot - 14530 Luc-sur-Mer, France

orianne.jolly@unicaen.fr; pascal.claquin@unicaen.fr

Abstract. Man-made infrastructures are wildly developed in many coastal ecosystems. Understanding and improving the positive interactions between concrete maritime infrastructures and biological components remains one of the ecological engineering challenges. The aim of this study is to evaluate the ability of a benthic diatom species, *Cylindrotheca closterium* (*C. closterium*), to use the mortar of artificial marine structure

as a silicon source for their own metabolism and growth. Diatoms are the dominant class of primary producer in many ecosystems. Diatoms need to absorb dissolved silica (dSi) in the form of $Si(OH)_4$ in order to synthesize their cell wall (the frustule). Batch cultures of *C. closterium* were performed under silicon limitation with or without the presence of mortar. First, the dissolution kinetics of silica from mortar in seawater were studied. Thereafter, the interaction between microalgae and dissolution kinetic properties were explored along with diatom biological parameters (Growth, biogenic silica per cell, biovolume, silicification degree and photosynthetic parameters). The dSi released by the mortar increases from the first days in the medium. Subsequently the $Si(OH)_4$ concentration decreased when microalgae were introduced into the medium associated to a parallel increase of the biogenic silica showing that cells are able to use dSi from the mortar to elaborate their frustule. The study also identified modifications of some of morpho-functional traits of *C. closterium* to maintain growth under limited Si conditions. This study shows how the benthic diatom *C. closterium* are able to benefit and acclimate from silica input provided by immersed artificial structures.

Keywords: marine ecology, *Cylindrotheca closterium,* mortar, silicon-limitation, bioavailability, pH, dissolution kinetics, biogenic silica.

1. Introduction

In the marine environment, cementitious materials are often used to create hard artificial structures. These have several applications for human activities, namely coastal protection, coastal development etc. These artificial structures represent new habitats for marine species and new approaches in eco-engineering [1–7] appearing to promote positive interactions between the biological compartment and the cement matrix. The

cementitious materials are bio-receptive in the marine environment [8]. Indeed, this hard substrate is immediately covered by a thin layer of biofilm, which is the first phase of biological settlement. The biofilm is composed of a succession of benthic communities (mostly diatoms [9]) which favor the second phase of settlement with macro-algae and other sessile organisms [9,10]. The surface heterogeneity and composition of artificial structures determine specific benthic biological community recruitment [6,11].

Diatoms are important functional components of marine benthic ecosystems [12]. They are eukaryotic unicellular photosynthetic microorganisms and are the dominant class of primary producers in many coastal ecosystems. They are characterized by a silica cell wall, frustule which consists essentially of hydrated amorphous silica (bSi associated with organic components [13]). Diatoms need dissolved Si (dSi) in the form of orthosilicic acid ($Si(OH)_4$) (97% of total dSi in natural seawater) to grow and form their frustule [14,15]. Concentrations of dSi vary considerably in natural seawater, from 10 to 40 µM in the North Atlantic [16] and can be also limiting for diatoms growth in costal ecosystem before other nutrients [17].

Under optimal conditions, diatoms absorb nutrients in theoretical stoichiometric ratios of C:N:P = 106:16:1 [18] as well as orthosilicic acid in ratios of Si:N = 1 and Si:C = 0.09-0.13 [19]. Martin-Jézéquel et al.,[14] and Claquin et al.,[20] have showed that the silica metabolism and the resulting silicification degree of algal cells was influenced by nutrient availability and growth rate. Si limitation induces a decrease in the growth rate and Si starvation leads to an arrest of growth in G1 and G2 phases of the cell cycle [21]. Nutrient limitation leads to a variation in cell size, reflecting cell acclimatization. Leynaert et al., [22] shows that Si uptake parameters kinetics are related to cell size.

71 The aim of this study is to explore the interaction between cementitious material and a
72 diatom biofilm of *C. closterium* regarding their demand of Si for growth. The substrate
73 used is a cementitious mortar. The mortar is ideal for studying the cement matrix on a
74 small scale. Indeed, when a cement based material is immersed in the marine
75 environment, it is subjected to different types of physical, chemical [23–26] and
76 biological aggression [27] that can have an impact on its matrix. The development of a
77 biofilm on the mortar' surface can lead to bio-deterioration and chemical components
78 release [28].

79 The biological activity of diatoms will cause an acceleration of chemical species release
80 from the cementitious material into the surrounding environment through matrix
81 leaching. The quantity and the type of released ions varies depending on the cement
82 matrix constitution. Different studies demonstrated that micro- and macro-organisms
83 (macro-algae) can assimilate dissolved nutrients from the cement paste in the water
84 column [28–31].

85 In the present work, the capacity of the benthic diatom species *C. closterium*, to assimilate
86 the silica released by the mortar was investigated. A first step was devoted to investigate
87 whether the mortar was capable of releasing dSi in the form of $Si(OH)_4$. In a second step,
88 a laboratory experiment was performed to evaluate the possible benefit of the silica
89 dissolution from the mortar for diatoms growth. For that purpose, batch cultures of *C.*
90 *closterium* were performed under silica limitation with or without the presence of mortar.
91 The kinetics of diatoms growth and several physiological performances were
92 investigated.

93 **2. Materials and Methods**

2.1. Mortar samples

For this study, one type of mortar was made using cement (CEM II/A- LL 42.5 R CE PM-CP2 NF) and a 0/2 mm siliceous alluvial sand, with a water to cement ratio equal to 0.5. This type of cement is suitable for marine concrete structures. Mortar specimens were made in accordance with the EN 196-1 standard [32]. The Table 1 presents the quantities of materials used to manufacture the mortar specimens.

Table 1. Composition in kg for 1m^3 of mortar

Mortar composition		
Cement	Sand	Water
511	255	1532

The chemical oxide composition of the studied cement is given in Table 2. It contains 19.4 % of silica (SiO_2).

Table 2. Chemical oxide contents in % of the studied cement (Calcia)

SiO_2	Al_2O_3	Fe_2O_3	TiO_2	MnO	CaO	MgO	SO_3	K_2O	Na_2O	P_2O_5	S^-	Cl^-
19.4	4.5	3.8	0.3	0	63.7	1	2.6	0.86	3	0.3	0.1	0.03

40 mm x 40 mm x 160 mm samples were exposed to a Relative Humidity of 100 % for 24 hours, before being removed from the mould and stored in water for 90 days at room temperature. Subsequently, the samples were cut with a saw to 10 mm x 10 mm x 5 mm cubes. The colonized and studied sides correspond to the surfaces in contact with the polystyrene moulds.

2.2. Culture Condition of the marine diatom *C. closterium*

C. closterium (Ehrenberg) Reimann & J.C. Lewin 1964 was cultured semi-continuously in order to maintain the population in exponential growth phase. Cultures were grown at 19 °C and under a light/dark cycle (12 h: 12 h) in artificial seawater (sea salts dosed at 33.3 $g.L^{-1}$; (Instant Ocean©, Spectrum Brand)). This dosage allows to obtain a salt composition ($MgCl_2$, $MgSO_4$, NaCl, $CaCl_2$) close to that found on average in natural seawater [33]. This artificial seawater was enriched with Conway medium [34]. They were maintained in polycarbonate flasks and were constantly aerated and mixed, to prevent CO_2 limitation and cell sedimentation.

2.3. Experimental set-up

In order to understand the interaction between the mortar and the diatom *C. closterium*, the concentration of dSi, the diatoms growth and physiological parameters were measured under the four following different Conditions:

- Condition 1 (M+/Si-/Cc-): medium with Mortar (M+), without adding $Si(OH)_4$ (Si-), without *C. closterium* inoculum (Cc-) over 30 days,
- Condition 2 (M+/Si-/Cc+): medium with Mortar (M+), without adding $Si(OH)_4$ (Si-), with *C. closterium* inoculum (Cc+) over 15 days,
- Condition 3 (M-/Si+/Cc+): medium without Mortar (M-), with adding $Si(OH)_4$ (Si+), with *C. closterium* inoculum (Cc+) over 15 days,
- Condition 4 (M-/Si-/Cc+): medium without Mortar (M-), without adding $Si(OH)_4$ (Si-), with *C. closterium* inoculum (Cc+) over 15 days.

The comparison of Conditions 1 and 2 aims to evaluate whether the dissolution of the mortar (measured in Condition 1) supports the growth of diatoms (Condition 2) and to

evaluate the evolution of this interaction in time. Conditions 3 and 4 are controls for Conditions 1 and 2. Conditions 2 and 3 allow the comparison of diatom growth kinetics supported by mortar dissolution to a culture directly enriched with $Si(OH)_4$. Condition 4 allows the evolution of the growth of *C. closterium* to be evaluated under Si-deficient conditions. This condition compared to Condition 2 establishes the effect of the interaction between the mortar and the diatom.

Any external contamination by Si was prevented.

2.3.1. Immersion medium

Condition 1 (M+/Si-/Cc-): the mortar immersion medium contained artificial seawater [33] enriched with Conway medium [34] (free from silicate solution to produce Si-free artificial seawater) which is a nutrient source for the microalgae. The tests were carried out in triplicates. The mortar weight (g) to immersion medium volume (mL) ratio (w/v=0.023) has been maintained constant for all the tests.

Condition 2 (M+/Si-/Cc+) included the introduction of the microalgae, previously centrifuged in order to remove all previous culture medium, in Condition 1.

The control media: Condition 3 (M-/Si+/Cc+) and Condition 4 (M-/Si-/Cc+) did not contain mortar but only artificial seawater enriched with Conway's medium with or without adding $Si(OH)_4$ respectively. As described for Condition 2, the microalgae were first centrifuged and rinsed before being inoculated into Condition 3 and 4.

Cultures were grown at 19 °C and under a light/dark cycle (12 h: 12 h). At this stage, the culture dilutions were stopped, and they became “batch” cultures. the immersion seawater was regularly mixed (3 times every day).

2.4. *Dissolution kinetics of silica from mortar*

The dissolution kinetics of silica from mortar was studied for different durations according to the studied Condition. Indeed, the duration of the experimental phase was set to 30 days (day 1-2-3-6-9-12-15-20 and 30) for Condition 1. This wide time range made it possible to determine how long dSi (as $Si(OH)_4$) was available in solution to the microalgae. For the Conditions 2, 3 and 4, the experimental phase was conducted over 15 days (1, 2, 3, 6, 9, 12 and 15). This difference of duration between the conditions was explained in the results section.

After each duration, the $Si(OH)_4$ concentration of the immersion medium was measured using a Seal Analytical AA3 HR auto-analyzer [35] based on a colorimetric method. The range of $Si(OH)_4$ analyses was from 0 to 160 µmol/L with a detection limit of 0.05 µmol/L.

When algal cells were present in the medium, centrifuging was required before analysis. The net assimilation of dissolved silica by the diatoms was estimated daily.

2.5. Biogenic silica (bSi) concentration measurement

In order to evaluate the frustule formation, the bSi content per cell was measured. Cell concentration of the medium was estimated by cell counting using a Mallassez counting chamber and an optical microscope (Keyence VHX-6000 microscope) at a magnification of x150. After rinsing the cells in artificial seawater, the solution was centrifuged for 10 min (3000 rpm. 19 °C). The supernatant was discarded and the pellet was resuspended in 10 mL of NaOH (0.2 M) to begin alkaline hydrolysis of biogenic silica for 45 min. The solution was stirred regularly to ensure the dissolution of all bSi [36] to $Si(OH)_4$. 1 mL of solution was diluted in 9 mL of MilliQ H_2O. The $Si(OH)_4$ concentrations (i.e. bSi

concentration) was determined using a Seal Analytical AA3 HR auto-analyzer. From this data, the bSi content per cell was calculated.

2.6. Cell surface and biovolume measurement

Cell dimensions were determined by imaging analysis using a Keyence VHX-6000 microscope (magnification x500). Biovolume (V) (equivalent to real biomass) was calculated from the mean of linear dimensions using the appropriate geometric formulae reflecting the shape of the cell [37]. The measurement of dimensions was carried out on 10 cells taken at random from the image captured under the microscope.

Calculation of cell volume was performed with the assumption of rotational ellipsoid shape using the Equation 1 [38]:

$$\text{Biovolume (V)} = \frac{\pi}{6} \times \text{ Height x Diameter}^2 \quad (1)$$

Where V is in μm^3 and H and D in µm.

The cell surface (S) was taken from Hillebrand et al., [37] (Equation 2):

$$\text{Surface (S)} = \frac{\pi D}{2} \times \left(D + \frac{H^2}{\sqrt{H^2 - D^2}} \sin^{-1} \frac{\sqrt{H^2 - D^2}}{H}\right) \quad (2)$$

Biovolume (V), surface area (S) and S/V ratio (considered a combined measure of size and shape) are parameters related to the productivity and microalgae metabolism.

2.7. Chlorophyll *a* extraction

Chlorophyll *a* (Chl *a*) extractions were made from biofilm samples on mortar after 1 day of incubation in Condition 2 (M+/Si-/Cc+). The biofilm was sampled using a smooth toothbrush on the mortar surface, then diluted in 10 mL of artificial sea water ($33.3 g.L^{-1}$). 10 mL of an analytical grade acetone were added for the pigment extraction and samples

were left 12 h in darkness at 4°C. After two centrifugations for 5 min at 1700 g, the Chl *a* concentration of the extracts was measured using a Trilogy fluorimeter (Turner Designs, Sunnyvale, USA) according to the Strickland and Parsons, (1972) method [39].

These data allowed us to estimate a factor between F_0 (chlorophyll biomass index) and Chl *a* ($\mu g.m^{-2}$) calculated on 3 samples. The calculated conversion factor was:

$$\frac{F_O}{Chl\ a} = 3.14 \quad (3)$$

This ratio enabled the estimation of the amount of Chl*a* for each sample each day from the F_0 obtained during the Pulse Amplitude Modulation (PAM) fluorescence (section 2.8).

2.8.Photosynthetic measurements

Photosynthetic parameters of mortar biofilms were assessed using PAM measurements. The maximum quantum yield of PSII (F_v/F_m) is widely used as an indicator of the nutrient stress of microphytobenthos cells [40]. To perform these measurements a Junior PAM (Walz Teaching-PAM fluorometer) with an optic fibre 50 cm long and 1.5 mm of diameter was used. After 10 min of dark acclimation, the photosynthetic parameters measurements were performed directly on the material surface regularly throughout the experiment. The sample was excited by a weak blue light (1 $\mu mol.photons.m^{-2}.s^{-1}$, 450 nm, 5 Hz) to record minimum fluorescence (F_0). The minimum fluorescence (F_0, basic fluorescence) is an index of chlorophyll biomass estimated after a dark acclimation largely used [41-42]. Maximum fluorescence (F_m) was obtained using a saturating light pulse (0.6s. 1500 $\mu mol.photons.m^{-2}.s^{-1}$. 450 nm) allowing all the Q_A pool to be reduced. F_v/F_m ratio was calculated according to Equation 4 [43]:

$$\frac{F_v}{F_m} = \frac{(F_m - F_0)}{F_m} \quad (4)$$

The samples were exposed to nine irradiances (E) from 0 to 420 µmol photons m^{-2} s^{-1} for 80 s at each step. Thus, steady-state fluorescence (F_s) and maximum fluorescence (F_m') were measured for each irradiance. The relative ETR (rElectron Transport Rate) is calculated according to Equation 5:

$$rETR(E) = \frac{F_m' - F_s}{F_m'} \times \mathrm{E} \quad (5)$$

To estimate the photosynthetic parameters, the rETR values were plotted as light response curves (photosynthetic rate (P) vs. light intensity or irradiance (E, µmol.photons.m^{-2}.s^{-1})). The mechanistic model developed by Webb et al.,[44] applied to fit the data to estimate α (µmol electrons.µmol photons^{-1}) and Ek (µmol photons.m^{-2}.s^{-1})) with α the initial slop of the FLC and Ek the light saturation index (equation 6):

$$rETR = \alpha \times \mathrm{Ek} \times (1 - e^{-\frac{E}{Ek}}) \quad (6)$$

Then the maximum of relative Electron Transport Rate ($rETR_{max.}$ µmol electrons.m^{-2}.s^{-1}) was calculated in accordance with Equation 7:

$$rETR_{MAX} = \alpha \times Ek \quad (7)$$

2.9. pH measurements

A monitoring of immersion medium pH was carried out throughout the experiment (one measurement one measurement per day) using a pH 510 meter (Eutech instrument). These measurements were undertaken in order to evaluate the effect of pH on silica dissolution kinetics.

3. Data analyses

Repeated measures ANOVA (RM ANOVA) were performed using SigmaPlot 12.5 (Systat Software Inc. Chicago, USA) followed by pairwise multiple comparison (Tukey's

235 test) when normality Shapiro-Wilk and equal variance (homoscedasticity) tests
236 respectively applied passed (>0.05). When normality or equal tests failed (<0.05), a
237 Friedman repeated measures analysis of variance on ranks was applied followed by
238 pairwise multiple comparison (Tukey's test). Differences were considered significant
239 when the p-value was less than 0.05. All plots and linear regressions were performed
240 using SigmaPlot 12.5.

241 **4. Results**

242 **4.1. Dissolution of the silica from the mortar without and with microalgae**

243 Fig. 1a shows the dissolution kinetics of silica from mortar in Condition 1 (M+/ Si-/Cc-).
244 The dSi concentration increased in the medium reaching its maximum after 2 days with
245 a value of 99.84 µmol.L^{-1}. From the 2nd day, the concentration of dissolved silica
246 decreased until it reached values below 18.68 µmol.L^{-1} after 6 days of experimentation.
247 dSi was no longer available in the medium at the end of the experiment. i.e. on day 30
248 (1.89 µmol.L^{-1}) with pH increasing until the end of the experiment with a pH of 9.7 at
249 day 30.

250 Fig. 1a shows also the dissolution kinetics of the Silica from the mortar once the
251 microalgae have been introduced into the medium (Condition 2, (M+/Si-/Cc+)). The
252 concentration of dSi increased during the first 2 days (11.39 µmol.L^{-1} and 21.51 µmol.L^{-1}
253 at day 1 and 2 respectively) and then decreased from day 3 onwards until values below
254 9.82 µmol.L^{-1} were reached. Indeed, the dSi concentrations were much lower in
255 Condition 2 (M+/Si-/Cc+) than in Condition 1 (M+/Si-/Cc-).
256 Fig. 1b shows the dSi content available in the Condition 3 (M-/Si+/Cc+) and Condition 4
257 (M-/Si-/Cc+) control medium. Initially, the Si non-limited control medium (Condition 3,
258 M-/Si+/Cc+) contained 190 µmol.L^{-1} of dSi (contained in the Conway medium). As in

Condition 2 (M+/Si-/ Cc+), the quantity of dSi decreased to 0 after 9 days. Diatoms gradually assimilated the dSi available in the medium until it was completely consumed. The dSi in Si-limited control medium (Condition 4, M-/Si-/Cc+) (Fig. 1b) was around 0. This result confirmed that the studied medium was Si-free. According to the Friedman test, we observed a significant difference (P = <0.001) in dSi concentration in the different Condition. Tukey test revealed that there was no significant difference between Conditions 1 and 3 and between Conditions 1 and 2 (P = 0.405).

A significant increase in pH, from 7.74 (Day 0) to 9.1, was observed after three days of experiment in Condition 1 (M+/Si-/Cc-) (Fig. 1a). The pH evolution in Condition 2 (M+/Si-/Cc+) followed the same trend than in Condition 1 (M+/Si-/Cc-) (Fig. 1a) with pH= 8.2 and pH=9.6 at respectively Day 0 and Day 3. Then, it could be noticed that a more alcaline pH was reached in Condition 2. After 9 days a stabilization of pH values was registered for both Conditions.

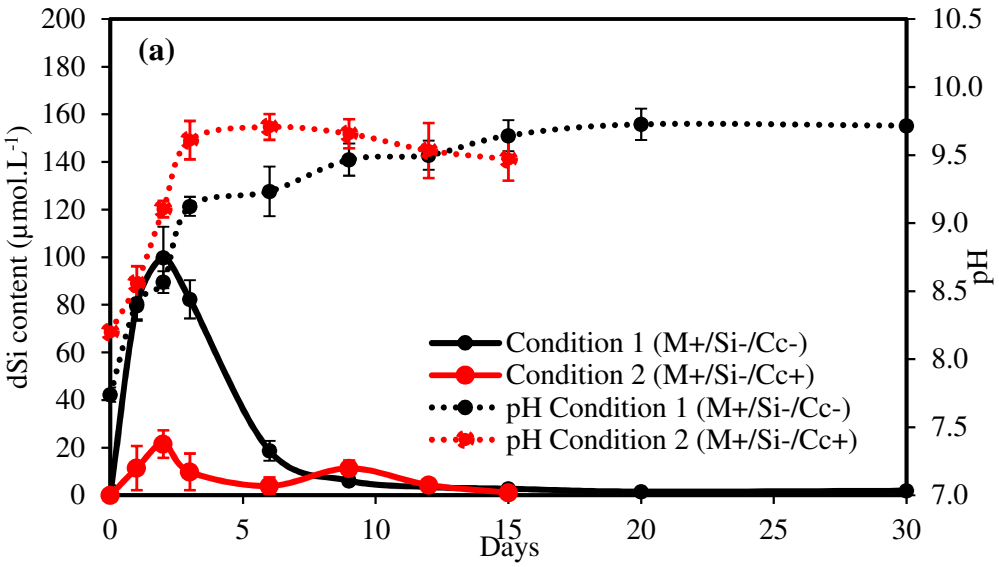

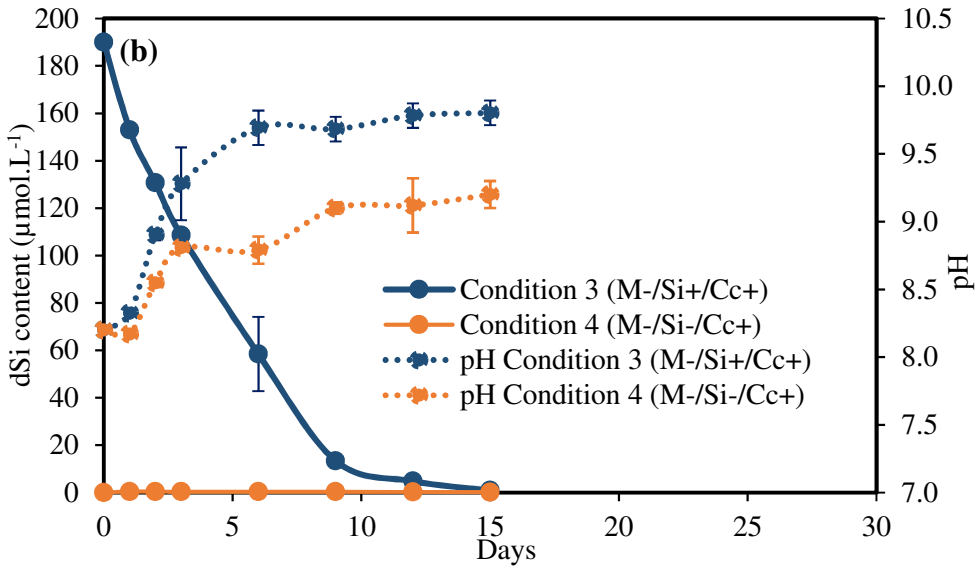

272 **Fig. 1.** Dissolution kinetics of mortar silica (solid line) and pH (dotted line) in
273 Condition 1 (M+/Si-/Cc-) and in Condition 2 (M+/Si-/Cc+) (with the microalgae) **(a)**,
274 dSi content and pH in Condition 3 (M-/Si+/Cc+) and Condition 4 (M-/Si-/Cc+) control
275 **(b)**. Means ± range of three replicate are shown.
276
277 In the control Conditions (3 and 4) (Fig. 1b), the pH also increased gradually in the
278 medium during the experiment, not exceeding 9.2 for Condition 4, in contrast to
279 Condition 3 where a pH increased up to 9.8 was observed. The Friedman test showed a
280 significant difference (P = <0.001) in pH in the different Conditions. Tukey tests revealed
281 that pH in media was no significantly different between Condition 2 and 3 and between
282 Condition 3 and 1 from the others.
283 From the measurement of the dSi concentration in the solution, it was possible to estimate
284 the concentration of dSi absorbed by the diatoms during the experiment. Fig.2 shows the
285 evolution of the assimilated silica per day by *C. closterium* in Condition 2 (M+/Si-/Cc+)
286 as function of experimental duration. We determined that silica assimilation by diatoms

in the $Si(OH)_4$ form was very high during the first 3 days with an average of 73 ±5 µmol.L^{-1}.j^{-1} (Fig.2). The assimilated quantity of silica was maximum at Day 2 with 78 µmol.L^{-1}.j^{-1} then decreased progressively until zero value. Thus, it could be concluded that the microalgae had consumed all the available dSi in the medium.

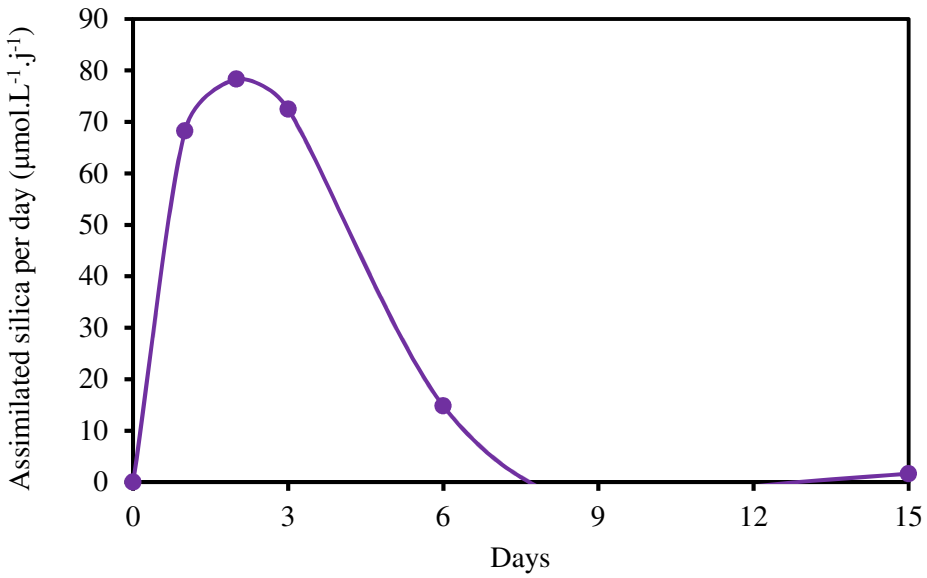

Fig. 2. Assimilated silica per day of *C. closterium* in Condition 2 (M+/Si-/Cc+).

4.2. Growth of *C. closterium* cells

4.2.1. Cell density and biogenic silica (bSi)

The growth of *C. closterium* showed an initial lag-phase (day 1, 2 and 3), followed by an exponential phase that lasted until about day 6 (Fig. 3a) in Condition 2. Maximum cell concentration was 1.59. 10^9 cells. L^{-1} after this period. Cells density started to decline the last days of experiment.

The growth of *C. closterium* led to an increase in biogenic silica from the first day of experimentation (Fig. 3b). Indeed, in Condition 2 (M+/Si-/Cc+), bSi concentration was initially equal to 1176 µmol.L^{-1} and reached the value of 1303 µ.mol.L^{-1} on day 6.

In Condition 3 (M-/Si+/Cc+), the cells density increased slightly after one day of the experiment. A decline in the number of cells was observed after day 2 and 6. A peak in the cell number was observed in the medium on day 9 reaching a total of 1.68. 10^9 cells. L^{-1}.

RM ANOVA showed that there was a significant difference (P = <0.001) in different media. Tukey tests informed us that for cells density, there was no significant difference between Condition 2 (M+/Si-/Cc+) and Condition 3 (M-/Si+/Cc+). In contrast, there were a significant effect of dSi availability in cells density in Condition 4. Indeed, microalgae did not develop in the Si-limited control medium (Condition 4 (M-/Si-/ Cc+)).

The Friedman test showed that there was a significant difference (P = 0.016 < 0.050) on the bSi content (µmol.L^{-1}) between Condition 2 and Condition 3. Similarly, the Tukey test also showed that there was a significant difference (P<0.050)

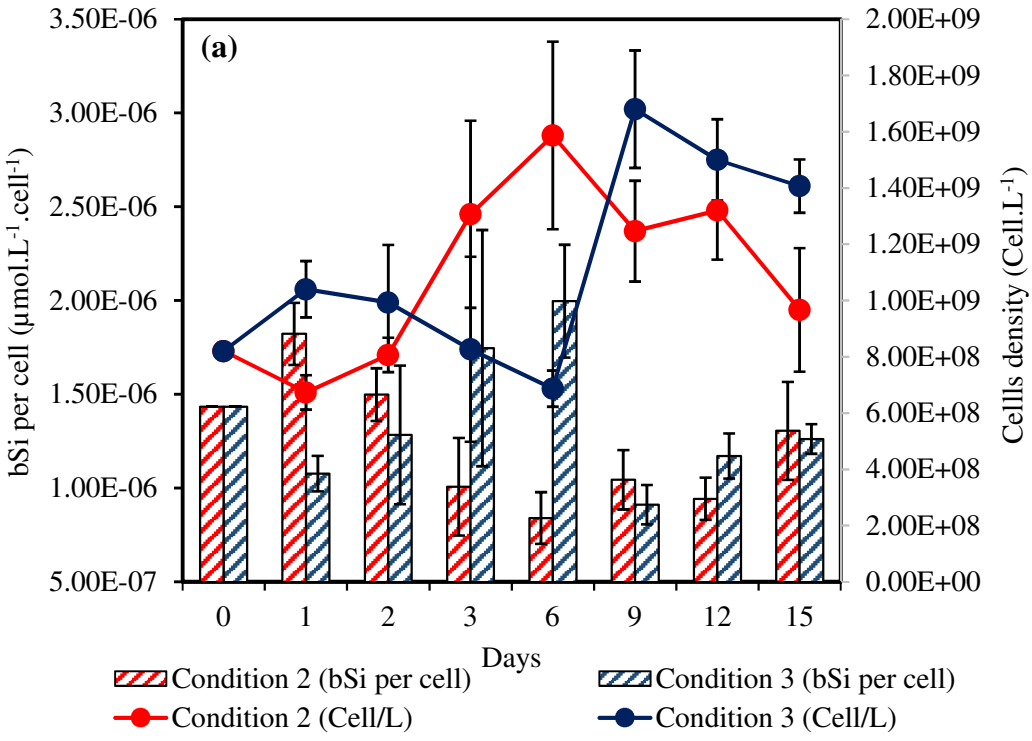

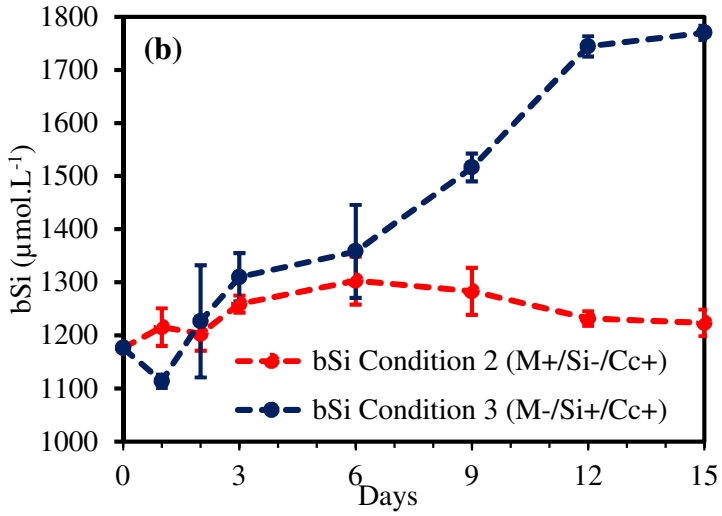

315

316 **Fig. 3.** Density of cells (cell.L^{-1}) of *C. closterium* and bSi content per cell

317 (µmol.L^{-1}.cell^{-1}) **(a)** ; Concentration of bSi (µmol.L^{-1}) **(b)** as a function of days in the

318 Condition 2 and 3**.**

319 The bSi content per cell was variable during culture growth (Fig. 3a). Indeed, in

320 Condition 2 (M+/Si-/Cc+), the frustule-bound bSi content per cell was initially equal to

321 $1.43.10^{-6}$ µ. mol.L^{-1}.cell^{-1} and achieved a value of $1.30.10^{-6}$ µ. mol.L^{-1}.cell^{-1} the last day.

322 The maximum bSi content per cell was registered at day 1 with a value of $1.82.10^{-6}$

323 µ.mol.L^{-1}.cell^{-1} (Fig. 3a). The silica content per cell was relatively stable from the 3rd day

324 with an average of $1.02.10^{-6}$ µ.mol.L^{-1}.cell^{-1}.

325 According to the RM Anova test, there was no statistically significant difference (P =

326 0.337) on bSi content per *C. closterium* cells (µmol.L^{-1}.cell^{-1}) between Condition 2 and 3.

327 The differences between the mean values of the amount of bSi content per cell in

328 conditions 2 and 3 was not large enough to exclude the possibility that the difference is

329 due to random sampling variability.

330 In Condition 3, the bSi per cell was very high at day 3 and day 6 reaching a value of

331 $1.74.10^{-6}$ µ.mol.L^{-1}.cell^{-1} and a value of $1.99\ 10^{-6}$ µ.mol.L^{-1}.cell^{-1} respectively. These

results had associated with a relatively low cell density in the culture media suggesting an increase in cell cycle duration. The formation of daughter cell valves in the mother cell took place between day 1 and 2 in Condition 2 and between day 3 and 6 in Condition 3, explaining the increase in the amount of bSi per cell (Fig. 3a). From day 3 for Condition 2 and day 9 for Condition 3, an increase in the amount of cells in the medium (Fig. 3a) was observed due to cell division and thus the separation of daughter cells from the mother cell. Thus, daughter cells were present in large quantities in the culture. The separation of the daughter cells explained the decrease in the quantity of bSi per cell with a value of $1.7.10^{-6}$ µ.mol.L^{-1}.$cell^{-1}$ on day 3 for condition 2 and $9.1.10^{-7}$ µ.mol.L^{-1}.$cell^{-1}$ on day 9 for Condition 3. From these times, the quantity of dissolved silica in the medium was very low (Fig. 1ab), causing the diatoms to stop growing (Fig. 3).

Indeed, from the 6^{th} day, very few cells in suspension were observed in the water column. Many algal cells aggregated and then settled to the bottom. The cells aggregates may form as a result of a limitation in nutrient. This observation has been confirmed by microscopic observations (Fig. 4). The cells aggregates were more frequent in Condition 4 (M-/Si-/Cc+) than in the other culture media.

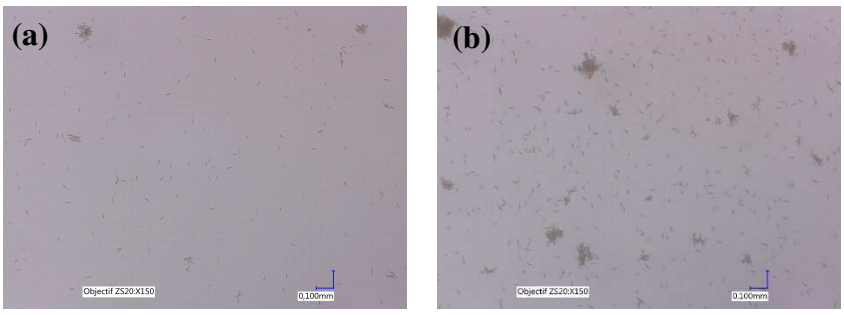

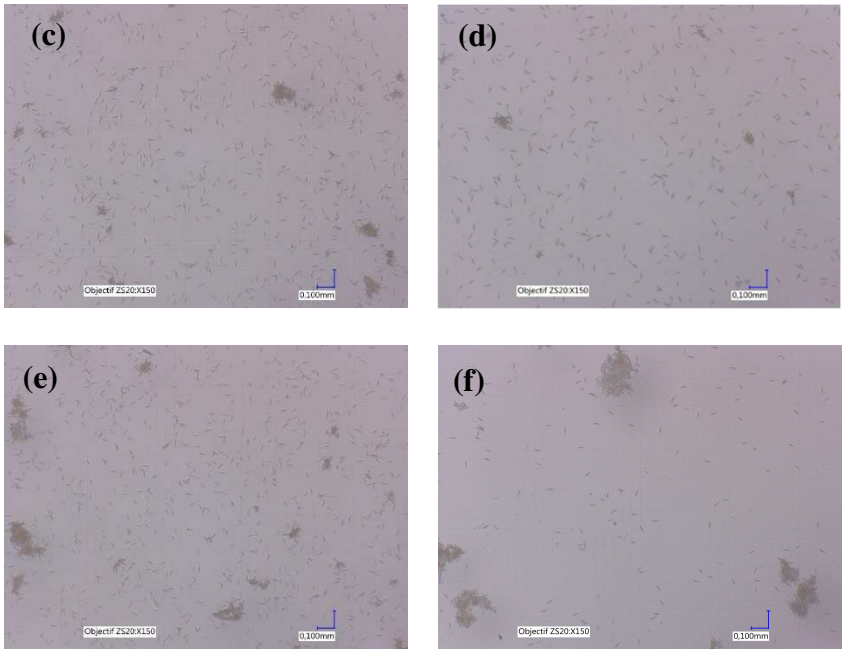

Fig. 4. Optical microscope observations (objective x20 - magnification x150) of *C. closterium* at Day 1 **(a)**, Day 3 **(b)**, Day 9 **(c)**, Day 15 **(d)** in Condition (M+/Si-/Cc+) and at Day 15 in Si non-limited (M-/Si+/Cc+) **(e)**, limited (M-/Si-/Cc+) **(f)**.

Fig. 5. shows optical microscope observations of *C. closterium* chloroplasts (where photosynthesis takes place) in the medium in Condition 2 (M+/Si-/Cc+) at Day 0 (Fig. 5a) and at Day 15 (Fig. 5b). A dyspigmentation of the chloroplasts was clearly visible under Si limitation.

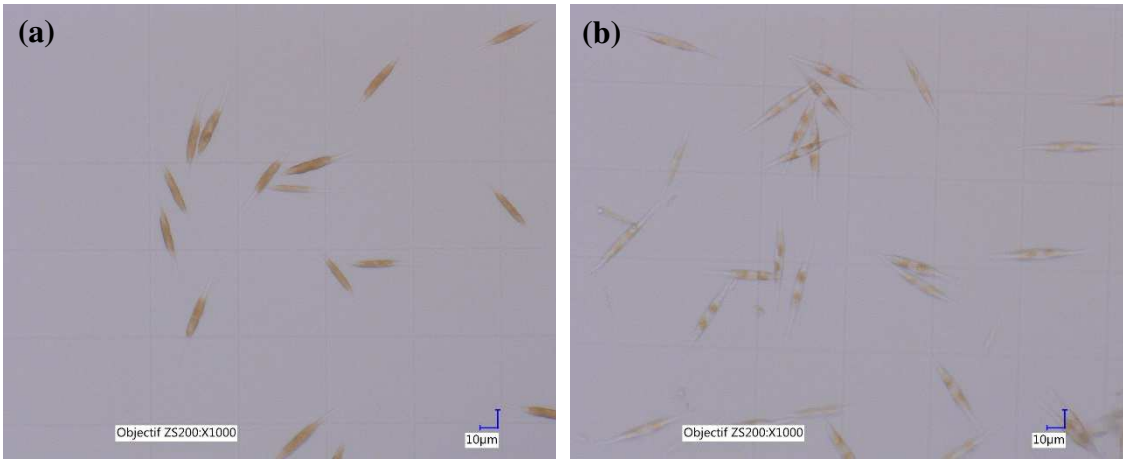

Day 0 **Day 15**

Fig. 5. Microscopic observation (objective x200 - magnification x1000) of *C. closterium* chloroplasts in the initial solution at Day 0 **(a)** and at Days 15 **(b)** in Condition 2 (M+/Si-/Cc+).

4.2.2. Biovolume

The large variation in size and shape of diatoms was shown by morphometric measurements represented in Table 3. The diameter and length of *C. closterium* were equal to 5.6 and 57.1 µm respectively in Condition 2 (M+/Si-/Cc+) and 5.2 and 57.2 µm in control media at Day 0. In Condition 2 (M+/Si-/Cc+), the diameter of the frustule (Table 3) decreased with time from 5.6 µm (Day 0) to 5 µm (Day 15). The same behavior was observed for Condition 3 (M-/Si+/Cc+) with values decreasing from 5.2 µm to 4.6 µm at Day 15. However, in the control medium Condition 4 (M-/Si-/Cc+), the frustule diameter remained stable at 5.2 µm.

The evolution of cell volume (Biovolume) and Surface/Volume ratio (S/V) for *C. closterium* are also presented in the Table 3. Regarding the cells biovolume, it decreased during the experiment from 989 μm^3 at Day 0 to 787 μm^3 the last day in Condition 2 (M+/Si-/Cc+) and from 809 μm^3 at Day 0 to 645 μm^3 at Day 15 in

379 Condition 3 (M-/Si+/Cc+). The biovolume of diatoms in Condition 4 (M-/Si-/Cc+)
380 showed relatively stable values over the experiment with values close to 820 ±54 µm^3.

381 **Table 3.** Mean values of linear measurements, n =10, Length, Diameter, biovolume (V)
382 and cell surface (S) of *C. closterium* cells.

Medium	Days	Length (µm)	Diameter (µm)	V (µm^3)	S (µm^{-2})
Condition 2 (M+/Si-/Cc+)	0	57.1 (±3.8)	5.7 (±0.7)	989 (±278)	809 (±130)
	1	55.1 (±2.4)	5.6 (±0.7)	917 (±238)	765 (±101)
	3	56.3 (±4.6)	5.2 (±0.6)	815 (±236)	728 (±129)
	9	56.1 (±5.1)	5.1 (±0.8)	727 (± 215)	683 (±138)
	15	55.0 (±2.0)	5.0 (±0.6)	787 (±180)	708 (±83)
Condition 3 (M-/Si+/Cc+)	0	57.2	5.2	809	736
	1	58.0 (±2.1)	5.2 (±0.4)	829 (±169)	748 (±85)
	3	57.2 (±2.1)	4.9 (±0.3)	722 (±90)	694 (±52)
	9	58.0 (±2.4)	4.5 (±0.7)	607 (±159)	638 (±95)
	15	57.7 (±2.0)	4.6 (±0.5)	645 (±137)	656 (±72)
Condition 4 (M-/Si-/Cc+)	0	57.2	5.2	809	736
	1	56.8 (±2.0)	5.2 (±0.6)	840 (±156)	748 (±85)
	3	57.9 (±1.7)	5.2(±0.7)	894 (±176)	777 (±79)
	9	57.7 (±2.1)	5.0 (±0.4)	745 (±110)	708 (±66)
	15	57.1 (±2.1)	5.2 (±0.4)	813 (±141)	735 (±65)

383

384 Fig. 6 shows the evolution of bSi per cell surface (Fig. 6a) and the S/V ratio (Fig. 6b) in
385 Condition 2 (M+/Si-/Cc+) and 3 (M-/Si+/Cc+) as function of experiment duration. A
386 decrease in the degree of silicification of the diatoms (Fig.6a) associated with a decrease
387 in the concentration of dSi (Fig.1) in both media was observed during the experiment. In
388 condition 2, the cells were more silicified during the first days of the experiment than
389 from day 3, going from 2.46. 10^{-9} µmol.bSi.µm^{-2} on day 1 to 1.4. 10^{-9} µmol.bSi.µm^{-2} on

day 3. The same trend was observed for cells grown in condition 3 with an increase in silicification of the cells until day 3 with a value of 2.5. 10^{-9} µmol.bSi.µm^{-2}. Indeed, silicon uptake by diatoms was higher in condition 3 during the first 3 days due to a higher silicon concentration in the medium.

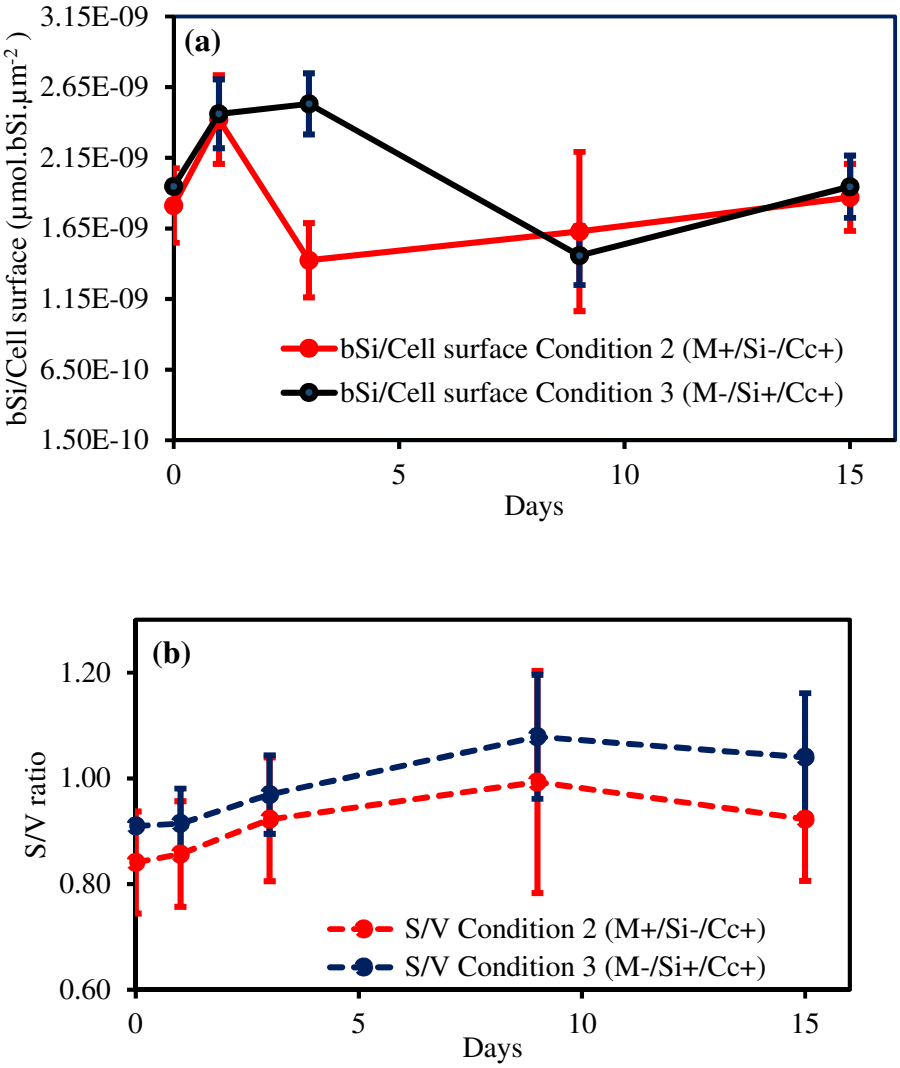

Fig. 6. bSi per cell surface **(a)** and the S/V ratio **(b)** in Condition 2 (M+/Si-/Cc+) and 3 (M- /Si+/Cc+).

The results showed that the mean S/V ratio increases gradually during the experiment from 0.84 initially to 0.92 the last day in Condition 2 (M+/Si-/Cc+) and from 0.91 initially to 1.04 the last day in Condition 3 (M-/Si+/Cc+).

In Condition 4 (M-/Si-/Cc+), the S/V ratio was relatively stable over the experiment (around 0.91). As the micro-algae did not develop, their morphological traits remained the same as at Day 0.

4.2.3. PAM measurement

Microscope observations illustrate the bio-colonization state of mortar after different experiment durations (Fig. 7), which follow the biofilm formation. Clearly not all mortar triplicates were uniform in terms of the algal biomass attached to their surface.

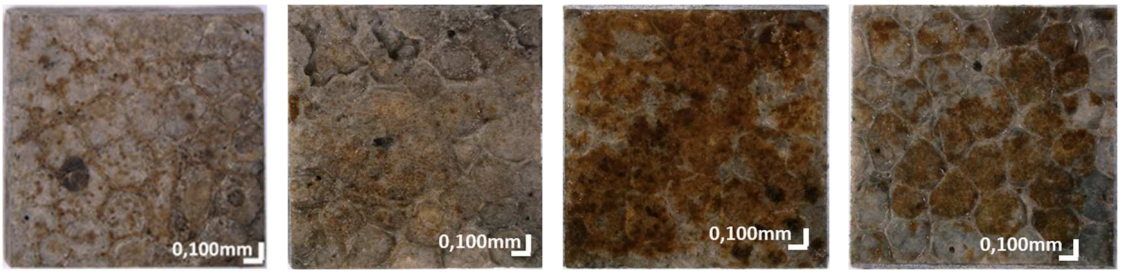

Day 1 **Day 3** **Day 9** **Day 15**

Fig. 7. Microscopic observations (objective x20 - magnification x150) of mortar at Day 1, Day 3, Day 9 and Day 15. Honeycomb-like structures are only a signature of the mortar to polystyrene mould contact.

Measurements of photosynthetic parameters and biofilm biomass on the surface of the material were made at each deadline. It should be pointed out that these measurements only represent a state of biocolonisation at a given point in time and not the total amount of biomass grown over the achieved period. Indeed, a part of biofilm was able to detach

itself from the surface, somehow compensated by new cell formation which accumulate to form biofilm again.

Fig. 8a showed the evolution of the biomass fixed on the mortar. It could be seen that the colonization of the mortar evolves over the course of the experiment (Fig. 7 and Fig. 8a).

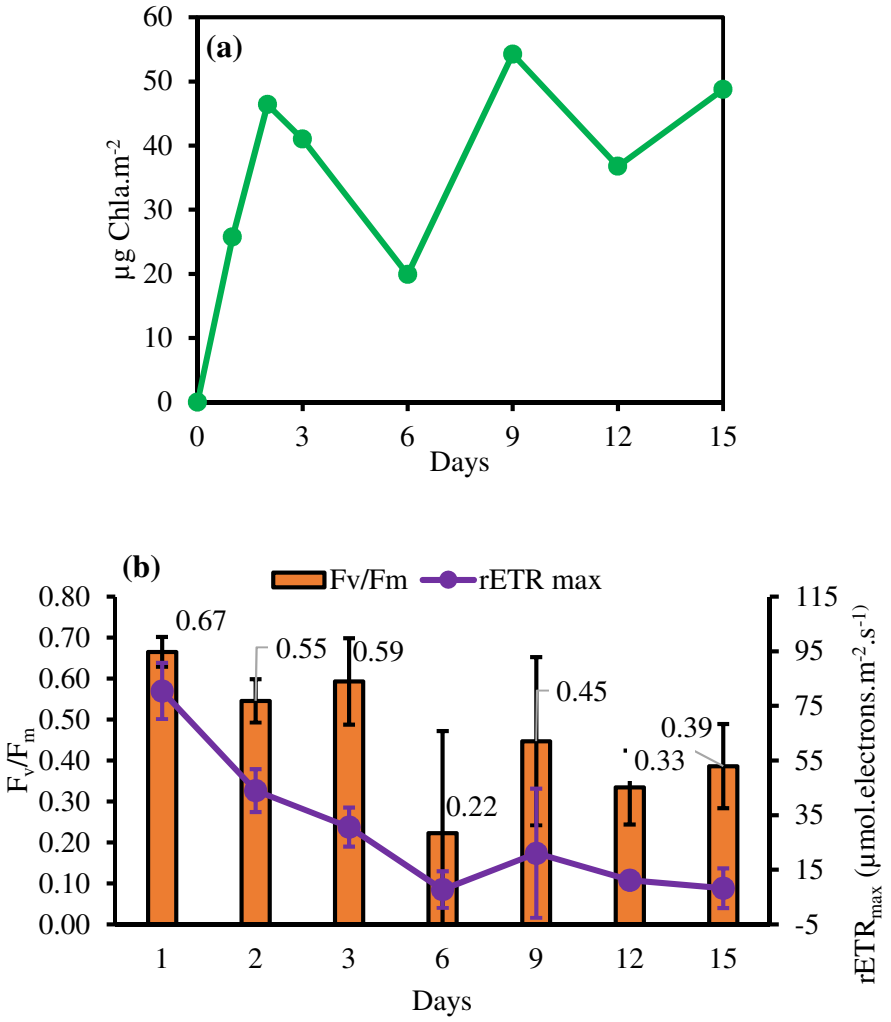

Fig. 8. Dynamics of microphytobenthic biofilm colonization on mortar as a function of time: Chlorophyll biomass per surface **(a)**; Average of F_v/F_m index maximum quantity efficiency of PSII (i.e. Physiological Status Index) **(b).**

The chlorophyll biomass increased from the first few days (maximum 46.4 µg.m^{-2} on day 2) then a fluctuation of the biomass is observed from day 6, reaching its maximum on day

9 with 54.2 µg.m^{-2}. The evolution of the Fv/Fm ratio as a function of time (Fig. 8b) indicated that microalgae were in good physiological state, with an average ratio of 0.43. On Day 6, the F_v/F_m ratio was the lowest (0.22±0.3) and around zero within the uncertainties, compared to the other days.The photosynthetic capacity ($rETR_{max}$) (Fig. 8b) showed a better electron transport rate during the first two days of the experiment with 80.47±10 and 43.99±8 µmol.electrons.m^{-2}.s^{-1}. A progressive decrease in photosynthetic capacity was observed over the immersion period to minimum values at Day 6 and Day 15 (7.72±7 and 8.23±7µmol.electrons.m^{-2}.s^{-1} respectively).

5. Discussion

5.1. *Dissolution of the silica from the mortar with and without the presence of microalgae*

Silica dissolution kinetics from the mortar showed a high concentration of dSi for the first few days. The dissolution rate of amorphous silica increased with pH [45], which explains the increase of dSi concentration in Condition 1 (M+/Si-/Cc-) during the first days of the experiment. The dSi concentrations obtained exceeded the silicate half saturation constant (K_μ) of *C. closterium* which is equal to 9.58 µmol.L^{-1} [46]. Therefore, in the first days of Condition 2, according to dSi concentrations, Si should be available for diatoms at a high uptake rate. Indeed, a modification of the Silica dissolution kinetics in Condition 2 (M+/Si-/Cc+) was observed. These results indicated that the *C. closterium* diatoms were able to assimilate the dSi, from the mortar for their metabolism.

The effects of the marine environment on cementitious materials are multiple and impact their durability [24]. Mortar will gradually leach out as a result of its reaction with the various chemicals in seawater. The silica dissolution from the mortar could be attributed

445 to the decalcification of the hydrated mineral phase: C-S-H (Calcium Silicate Hydrate)
446 (Equation 8) [47]. Indeed, the decalcification of C-S-H leads to SiO_2 release and $CaCO_3$
447 formation. Furthermore, at seawater pH values, the silica siloxane bonds were hydrolyzed
448 [48] leading to its dissolution as dSi forms (Equation 9).

$$C - S - H + 2CO_2 \rightarrow SiO_2 + 2CaCO_3 + H_2O \quad (8)$$

$$SiO_2 + 2H_2O \rightarrow Si(OH)_4 \quad (9)$$

449 In Condition 1 (M+/Si-/Cc-), a progressive decrease of the dSi concentration was
450 observed, associated to the solution pH increased until the end of the experiment. The
451 increase in pH was due to the chemical attack of the mortar by the artificial seawater. This
452 attack favoured the dissolution of portlandite ($Ca(OH)_2$) leading to the increase of Ca^{2+}
453 and OH^- ions concentration in the solution [49] (equation 10).

$$Ca(OH)_2 \rightarrow Ca^{2+} + 2OH^- \quad (10)$$

454 The recorded decreased of the dSi concentration in Condition 1 was explained by the
455 solubility of the $Si(OH)_4$ form in the medium. Indeed, Dent Glasser and Kataoka [50]
456 explained that the various forms of silica varies depending on the temperature, pH, and
457 alkali ion composition. In aqueous solutions, several forms of dSi were observed , the
458 abundance of which depending on pH: $Si(OH)_4$, $SiO(OH)_3^-$, $SiO_2(OH)_2^{2-}$, $SiO_3(OH)^{3-}$ and
459 SiO_4^{4-} [49]. The complex equilibrium of different forms of dSi constitutes the basis of the
460 biogeochemical cycle of silicon in the ocean.
461 According to Sjöberg et al., [52], the acid-base reactions of $Si(OH)_4$ in saline solutions
462 (25°C, 0.6M NaCl) were :

$$Si(OH)_4 \leftrightarrow SiO(OH)_3^- + H^+ \quad pKa_{1=} 9.47 \ (11)$$

$$SiO(OH)_3^- \leftrightarrow SiO_2(OH)_2^{2-} + H^+ \quad pKa_{2=} 12.6 \ (12)$$

463 The orthosilicic acid form which was assimilated by diatoms was mostly present at pH
464 values below 9 [53,54]. Indeed, when the pH was larger than pKa_1 (9.47), the $Si(OH)_4$
465 dissociated to another form (equation 11-12). Thus, the increase in pH during the
466 experiment led to the formation of $SiO(OH)_3^-$ explaining the reduction of the $Si(OH)_4$
467 concentration in the medium.
468 In Condition 2 (M+/Si-/Cc+), the pH of the surrounding environment changed with the
469 leaching of the cement matrix induced by the biological activity of the biofilm and the
470 chemical seawater attack. Our results suggested that photosynthesis inducing carbon
471 dioxide fixation by microalgae led to a larger pH in the medium compared to a medium
472 without diatom [55].

473 ***5.2. Influence of dSi availability on microalgal growth and mortar colonization by***
474 ***the biofilm***

475 In order to explain the influence of dSi availability on microalgae growth in the medium,
476 the concentration of bSi and cells density have been assessed during the experiment and
477 compared with control conditions. In this study, the increase in bSi concentration
478 associated with an increase in cells density showed that the microalgae developed and
479 were able to elaborate their frustule as a result of the assimilation of the dSi in the medium.
480 In addition, the availability of dSi in the medium affected the rate of silica (bSi)
481 incorporation into the frustules and thus the cell cycle of the diatoms. Indeed, the
482 concentration of bSi per cell and the thickness of the frustule were regulated by the total
483 amount of Si absorbed directly determined by the duration of the cell cycle [56]. We
484 observed similar diatom growth kinetics in both cultures (condition 2 and 3). However,
485 the difference observed between the two conditions could only be explained by the fact

that the amount of silicon available in the medium was lower when the dissolved silica came from the mortar (at the scale of our laboratory tests) than in a culture directly enriched with dSi.

Capellacci et al., [57] studied the growth parameters of two diatom species under controlled culture conditions in the presence of different sources of silicon (crystalline or amorphous silica). Their study proved that diatoms had higher growth rate, cell density, and silicon assimilation rate when growth in crystalline silica medium than the other amorphous silica one.

It should be also be noted that microalgae acclimatized well to the environmental modifications, notably to the pH increase. Indeed, Hinga, [58] demonstrated that *C. closterium* could not grow when pH values were above 8.5 which was not the case in this study. Therefore, the pH was not the major limiting factor in the present study.

In Condition 2 (M+/Si-/Cc+), the dSi in the medium came only from the mortar. All the other elements necessary for diatoms growth were present in the medium. Thus, these results indicated that in this study the first limiting factor for the growth of *C. closterium* was silicon. Microscopic observations showed the formation of cell aggregates at the end of the experiment and in the silica limited medium (Condition 4). The partial dissolution of extracellular polysaccharides, secreted by the diatoms, is at the origin of the cohesion of the cells with each other leading to aggregates formation [59]. The bSi in the diatoms' frustule can dissolve when all the nutrients essential for their growth aren’t longer available in the surrounding environment. However, Moriceau et al., [60,61] showed that dissolution rates of biogenic silica (bSi) were reduced when diatoms were incorporated into the aggregates making them more sustainable.

509 The dSi availability influence on the mortar colonisation by the biofilm was investigated
510 by monitoring the photosynthetic parameters and Chl *a* biomass during the experiment.
511 The F_v/F_m ratio is an indicator of nutritional stress in algal cells. It could therefore be
512 assumed that the decrease in F_v/F_m after 6 days of immersion may be a consequence of
513 increased competition between diatoms for access to light or nutrients. In addition, the
514 dissolved silica available in the environment was almost around zero at this period
515 causing stress for the diatoms. The best development of biofilm registered on day 9 has
516 led to the creation of a micro-habitat allowing the species to acclimate to its growth
517 environment changes, which may explain the increase in F_v/F_m [62] despite low nutrient
518 concentration and high pH. However, the F_v/F_m will no longer reach the values obtained
519 during the initial phase of biofilm development.

520 The photosynthetic yields F_v/F_m and the maximal photosynthethic capacity $rETR_{max}$
521 decreased progressively throughout the experiment due to the limited amount of silicon.
522 Only a few studies dealt with the effect of Si limitation on photosynthesis. In a previous
523 study performed on two pelagic diatoms, Napoléon et al., [63] showed that photosynthetic
524 parameters were weakly influenced by Si limitation, but the limitation applied in the
525 present study was stronger. In addition, the decline on photosynthethic capacity may be
526 due to a decrease in light energy absorption as the cells adapt to reduce the amount of
527 pigment. Indeed, Jungandreas et al., [64] demonstrated that the reduction in chlorophyll
528 *a* was an acclimation to the decrease in growth rate. Since the diatom reduced the amount
529 of absorbed light energy required to maintain biomass synthesis. The photosynthetic
530 performance of *C. closterium* was thus disturbed by the environmental conditions of the
531 medium leading to cell acclimatization.

532 ***5.3. Influence of dSi availability on micro-algae morpho-functional traits***

The diameter of the diatoms frustule decreased progressively during the experiment. These results showed that diatoms were able to acclimatize to the availability of dSi by reducing the thickness of their frustule. This acclimation allowed the cells to continue to grow until the medium was depleted [21,65].

dSi depletion induced a decrease in cell volume all over the growth under silica-limited Condition 2 and 3 (M+/Si-/Cc+ and M-/Si+/Cc+). We have pointed out that diatoms can acclimatize to silicon limitation by decreasing cell size.

The diatom was able to regulate the silica content incorporated in its frustule according to the quantity of $Si(OH)_4$ available in the medium without affecting its growth. The silicon uptake occurs mainly during valve formation. The SITs play also a role in the cell silicification since they are involved in silica deposition in Silica Vesicle Deposition (SDV) [66]. The increase in the rate of silica production in frustules may be due to the increase in the duration of the G2+M phase in the diatom cell cycle [21,67]. The decrease in the amount of silica dissolved in the medium explains why the cells were less and less silicified during the experiment. Nevertheless, this did not prevent the growth of diatoms.

According to McNair et al [68], diatoms acclimatize to reduced silicon availability by thinning their frustules reducing the impact of reduced Si uptake rates on division rates. This thinning of frustules (smaller and thinner cells) could result in an increase in the S/V ratio as observed in our experiment. According to Bonato, [69], the cell surface to volume (S/V) ratio allows the cell to acclimate its ability to harvest light and nutrients under limiting conditions. The S/V ratio of *C. closterium* increased in response to an acclimation of these cells to low dSi concentration. The associated increase in S/V ratio and decrease in thickness of the cell may improve nutrient transporter sites [70] and uptake kinetics.

556 SIlicon Transporter proteins (SITs) are involved in the absorption and transport of silicon
557 within the cell [71]. The number and type of SITs per cell surface drive the Si uptake
558 capacities of diatoms [72]. The acclimation of *C. closterium* cells size can take up nutrient
559 more efficiently in limiting nutrients. Vanucci et al., [73] have also revealed a
560 modification of cells volume under nutrient-limited environment.

561 This leads us to conclude that the modification observed in the silicification degree and
562 specific morphological characteristics of pennate diatoms are a response to the
563 availability of silicon in the medium to enhance its uptake, transport into the cell and
564 deposition in the SDV responsible for the formation of new valves.

565 **Conclusion**

566 This study examined the influence of a siliceous mortar on the growth kinetics of
567 *C. closterium* under silicon limitation. Laboratory monitoring revealed that the diatom
568 was able to assimilate the dSi from the mortar.
569 The increase in pH played a role in the uptake rate of dSi by diatoms since it made dSi
570 (in the $Si(OH)_4$ form) unavailable to *C. closterium* from day 6 of the experiment.
571 *C. closterium* adjusted these morphological traits to improve the uptake and transport of
572 silicon into the cell. The diatom has assimilated the dSi present in the solution by storing
573 it in their valves leading to an increase in the degree of silicification. We can conclude
574 that the first limiting factor for the growth of *C. closterium* was the silicon concentration
575 in the medium.

576 In natural environment, the dSi from the dissolution of the mortar from hard artificial
577 structures will not be limited by pH because of water mass volumes and currents. Thus,

578 these structures would contribute to new sources of silicon that can be assimilated by
579 diatoms from the microphytobenthos and the phytoplankton.

580 This new approach would assist the restoration of primary producers bringing new trophic
581 resources for the development of marine fauna and flora on the substrate.

582 **Acknowledgements.** The authors would like to warmly thank Jérome Lecourt
583 (Engineer), CRISMAT/ENSICAEN Laboratory and Léo Chasselin (Assistant Engineer),
584 CREC Marine Station for their precious help. The authors would also like to thank the
585 Interreg FCE MARINEFF Project for the financial support of this research work.

586 **References**

587 [1] S.D. Bergen, S.M. Bolton, J. L. Fridley, Design principles for ecological
588 engineering, Ecol. Eng. 18 (2001) 201–210. https://doi.org/10.1016/S0925-
589 8574(01)00078-7.

590 [2] H.D. Dennis, A.J. Evans, A.J. Banner, P.J. Moore, Reefcrete: Reducing the
591 environmental footprint of concretes for eco-engineering marine structures, Ecol. Eng.
592 120 (2018) 668–678. https://doi.org/10.1016/j.ecoleng.2017.05.031.

593 [3] L.B. Firth, R.C. Thompson, K. Bohn, M. Abbiati, L. Airoldi, T.J. Bouma, F.
594 Bozzeda, V.U. Ceccherelli, M.A. Colangelo, A. Evans, F. Ferrario, M.E. Hanley, H. Hinz,
595 S.P.G. Hoggart, J.E. Jackson, P. Moore, E.H. Morgan, S. Perkol-Finkel, M.W. Skov,
596 E.M. Strain, J. van Belzen, S.J. Hawkins, Between a rock and a hard place: Environmental
597 and engineering considerations when designing coastal defence structures, Coast. Eng.
598 87 (2014) 122–135. https://doi.org/10.1016/j.coastaleng.2013.10.015.

599 [4] L.B. Firth, K.A. Browne, A.M. Knights, S.J. Hawkins, R. Nash, Eco-engineered
600 rock pools: a concrete solution to biodiversity loss and urban sprawl in the marine
601 environment, Environ. Res. Lett. 11 (2016) 094015. https://doi.org/10.1088/1748-
602 9326/11/9/094015.

603 [5] W.J. Mitsch, What is ecological engineering?, Ecol. Eng. 45 (2012) 5–12.
604 https://doi.org/10.1016/j.ecoleng.2012.04.013.

605 [6] S. Pioch, G. Relini, J.C. Souche, M.J.F. Stive, D. De Monbrison, S. Nassif, F.
606 Simard, D. Allemand, P. Saussol, R. Spieler, K. Kilfoyle, Enhancing eco-engineering of
607 coastal infrastructure with eco-design: Moving from mitigation to integration, Ecol. Eng.
608 120 (2018) 574–584. https://doi.org/10.1016/j.ecoleng.2018.05.034.

609 [7] E.M.A. Strain, C. Olabarria, M. Mayer-Pinto, V. Cumbo, R.L. Morris, A.B.
610 Bugnot, K.A. Dafforn, E. Heery, L.B. Firth, P.R. Brooks, M.J. Bishop, Eco-engineering
611 urban infrastructure for marine and coastal biodiversity: Which interventions have the
612 greatest ecological benefit?, J. Appl. Ecol. 55 (2018) 426–441.
613 https://doi.org/10.1111/1365-2664.12961.

614 [8] J.F. Marquez-Peñaranda, M. Sanchez-Silva, J. Husserl, E. Bastidas-Arteaga,
615 Effects of biodeterioration on the mechanical properties of concrete, Mater. Struct. 49
616 (2016) 4085–4099. https://doi.org/10.1617/s11527-015-0774-4.

617 [9] M.M. Salta, J.A. Wharton, Y. Blache, K.R. Stokes, J.-F. Briand, Marine biofilms
618 on artificial surfaces: structure and dynamics., Environ. Microbiol. 15 (2013) 2879–2893.
619 https://doi.org/10.1111/1462-2920.12186.

620 [10] O. Hung, V. Thiyagarajan (Rajan), R. Zhang, R. Wu, P.-Y. Qian, Attachment of
621 Balanus amphitrite larvae to biofilms originated from contrasting environments in Hong

622 Kong, Mar. Ecol.-Prog. Ser. - MAR ECOL-PROGR SER. 333 (2007) 229–242.
623 https://doi.org/10.3354/meps333229.

624 [11] N. Hanlon, L.B. Firth, A.M. Knights, Time-dependent effects of orientation,
625 heterogeneity and composition determines benthic biological community recruitment
626 patterns on subtidal artificial structures, Ecol. Eng. 122 (2018) 219–228.
627 https://doi.org/10.1016/j.ecoleng.2018.08.013.

628 [12] R.C. Thompson, T.A. Norton, S.J. Hawkins, Physical Stress and Biological
629 Control Regulate the Producer-Consumer Balance in Intertidal Biofilms, Ecology. 85
630 (2004) 1372–1382.

631 [13] M. Hildebrand, S.J.L. Lerch, R.P. Shrestha, Understanding Diatom Cell Wall
632 Silicification—Moving Forward, Front. Mar. Sci. 5 (2018).
633 https://doi.org/10.3389/fmars.2018.00125.

634 [14] V. Martin-Jézéquel, M. Hildebrand, M.A. Brzezinski, Silicon Metabolism in
635 Diatoms: Implications for Growth, J. Phycol. 36 (2000) 821–840.
636 https://doi.org/10.1046/j.1529-8817.2000.00019.x.

637 [15] V. Martin-Jézéquell, P.J. Lopez, Silicon — a Central Metabolite for Diatom
638 Growth and Morphogenesis, in: W.E.G. Müller (Ed.), Silicon Biominer. Biol. —
639 Biochem. — Mol. Biol. — Biotechnol., Springer Berlin Heidelberg, Berlin, Heidelberg,
640 2003: pp. 99–124. https://doi.org/10.1007/978-3-642-55486-5_4.

641 [16] P. Tréguer, N. D.M, V. A.J, D. D.J, B. Quéguiner, A. Leynaert, The silica budget
642 of the World Ocean: a re-estimate, Science. 268 (1995) 375–379.

643 [17] Y. Del Amo, B. Quéguiner, P. Tréguer, H. Breton, L. Lampert, Impacts of high-
644 nitrate freshwater inputs on macrotidal ecosystems. II. Specific role of the silicic acid
645 pump in the year-round dominance of diatoms in the Bay of Brest (France), Mar. Ecol.
646 Prog. Ser. 161 (1997) 225–237. https://doi.org/10.3354/meps161225.

647 [18] A.C. Redfield, B.H. Ketchum, F.A. Richards, The influence of organisms on the
648 composition of sea water., Ed., The Sea, Vol. 2, In M. N. Hill [ed.], 1963.

649 [19] M.A. Brzezinski, The Si:C:N RATIO of marine diatoms: interspecific variability
650 and the effect of some environmental variables1, J. Phycol. 21 (1985) 347–357.
651 https://doi.org/10.1111/j.0022-3646.1985.00347.x.

652 [20] P. Claquin, V. Martin-Jezequel, J. Kromkamp, M. Veldhuis, G. Kraay,
653 Uncoupling of silicon compared with carbon and nitrogen metabolisms and the role of
654 the cell cycle in continuous cultures of Thalassiosira pseudonana (Bacillariophyceae)
655 under light, nitrogen and phosphorus control, J. Phycol. 38 (2002) 922–930.
656 https://doi.org/10.1046/j.1529-8817.2002.t01-1-01220.x.

657 [21] M.A. Brzezinski, R.J. Olson, S.W. Chisholm, Silicon availability and cell-cycle
658 progression in marine diatoms, Mar. Ecol. Prog. Ser. 67 (1990) 83–96.

659 [22] A. Leynaert, E. Bucciarelli, P. Claquin, R.C. Dugdale, V. Martin-Jézéquel, P.
660 Pondaven, O. Ragueneau, Effect of iron deficiency on diatom cell size and silicic acid
661 uptake kinetics, Limnol. Oceanogr. 49 (2004) 1134–1143.
662 https://doi.org/10.4319/lo.2004.49.4.1134.

663 [23] U.H. Jakobsen, K. De Weerdt, M.R. Geiker, Elemental zonation in marine
664 concrete, Cem. Concr. Res. 85 (2016) 12–27.
665 https://doi.org/10.1016/j.cemconres.2016.02.006.

666 [24] F. Qu, W. Li, W. Dong, V.W.Y. Tam, T. Yu, Durability deterioration of concrete
667 under marine environment from material to structure: A critical review, J. Build. Eng. 35
668 (2021) 102074. https://doi.org/10.1016/j.jobe.2020.102074.

669 [25] M.Z.Y. Ting, K.S. Wong, M.E. Rahman, S.J. Meheron, Deterioration of marine
670 concrete exposed to wetting-drying action, J. Clean. Prod. 278 (2021) 123383.
671 https://doi.org/10.1016/j.jclepro.2020.123383.

672 [26] Y. Yi, D. Zhu, S. Guo, Z. Zhang, C. Shi, A review on the deterioration and
673 approaches to enhance the durability of concrete in the marine environment, Cem. Concr.
674 Compos. 113 (2020) 103695. https://doi.org/10.1016/j.cemconcomp.2020.103695.

675 [27] H.O. Stanley, C.D. Onwukwe, S.D. Peesor, Assessment of microalgae-influenced
676 biodeterioration of concrete structures, Niger. J. Biotechnol. 34 (2017) 19–23.
677 https://doi.org/10.4314/njb.v34i1.3.

678 [28] E. Bastidas-Arteaga, M. Sánchez-Silva, A. Chateauneuf, M.R. Silva, Coupled
679 reliability model of biodeterioration, chloride ingress and cracking for reinforced concrete
680 structures, Struct. Saf. 30 (2008) 110–129.
681 https://doi.org/10.1016/j.strusafe.2006.09.001.

682 [29] P. Hughes, D. Fairhurst, I. Sherrington, N. Renevier, L.H.G. Morton, P.C. Robery,
683 L. Cunningham, Microscopic study into biodeterioration of marine concrete, Int.
684 Biodeterior. Biodegrad. 79 (2013) 14–19. https://doi.org/10.1016/j.ibiod.2013.01.007.

685 [30] R. Javaherdashti, H. Nikraz, M. Borowitzka, N. Moheimani, M. Olivia, On the
686 impact of algae on accelerating the biodeterioration/biocorrosion of reinforced concrete:
687 A mechanistic review, Eur. J. Sci. Res. 36 (2009) 394–406.

688 [31] S. Jayakumar, R. Saravanane, Biodeterioration of Coastal Concrete Structures by
689 Marine Green Algae, Int. J. Civ. Eng. 8 (2010) 352–361.

690 [32] NF EN 196-1, Methods of testing cement — Part 1: Determination of strength.
691 September 2016., (n.d.).

692 [33] M.J. Atkinson, C. Bingma, Elemental composition of commercial seasalts, J.
693 Aquaric. Aquat. Sci. VIII 2. (1997) 39-43.

694 [34] J. Tompkins, M. DeVille, J. Day, M. Turner, Culture Collection of Algae and
695 Protozoa: Catalogue of Strains, Titus Wilson Son Ltd Kendal. (1995) p208.

696 [35] A. Aminot, R. Kérouel, Dosage automatique des nutriments dans les eaux
697 marines, méthodes en flux continu, Edition QUAE, 2007.

698 [36] O. Ragueneau, P. Tréguer, Determination of biogenic silica in coastal waters:
699 applicability and limits of the alkaline digestion method, Mar. Chem. 45 (1994) 43–51.
700 https://doi.org/10.1016/0304-4203(94)90090-6.

701 [37] H. Hillebrand, C.-D. Dürselen, D. Kirschtel, U. Pollingher, T. Zohary, Biovolume
702 Calculation for Pelagic and Benthic Microalgae, J. Phycol. 35 (1999) 403–424.
703 https://doi.org/10.1046/j.1529-8817.1999.3520403.x.

704 [38] I. Olenina, S. Hajdu, L. Edler, A. Andersson, N. Wasmund, S. Busch, J. Göbel, S.
705 Gromisz, S. Huseby, M. Huttunen, A. Jaanus, P. Kokkonen, I. Jurgensone, E.
706 Niemkiewicz, Biovolumes and size-classes of phytoplankton in the Baltic Sea, HELCOM
707 Balt Sea Env. Proc. 106 (2006).

708 [39] J.D.H. Strickland, A Practical Handbook of Seawater Analysis, 2nd Edition, 2nd
709 edition, Fisheries Research Board of Canada, 1972.

710 [40] P. Juneau, B.R. Green, P.J. Harrison, Simulation of Pulse-Amplitude-Modulated
711 (PAM) fluorescence: Limitations of some PAM-parameters in studying environmental
712 stress effects, Photosynthetica. 43 (2005) 75–83. https://doi.org/10.1007/s11099-005-
713 5083-7.

714 [41] J. Cosgrove, MA. Borowitzka. Chlorophyll fluorescence terminology: An
715 introduction. In: DJ. Suggett, O. Prasil, MA. Borowitzka, editors. Chlorophyll a
716 Fluorescence in Aquatic Sciences: Methods and Applications: Springer; (2010). p. 1-17.

717 [42] B. Vivier, P. Claquin, C. Lelong, Q. Lesage, M. Peccate, B. Hamel, M. Georges,
718 A. Bourguiba, N. Sebaibi, M. Boutouil, D. Goux, J.C. Dauvin and F. Orvain Influence of
719 infrastructure material composition and microtopography on marine biofilm growth and
720 photobiology, Biofouling, 37:7(2021) 740-756.
721 https://doi.org/10.1080/08927014.2021.1959918

722 [43] B. Genty, J.-M. Briantais, N.R. Baker, The relationship between the quantum
723 yield of photosynthetic electron transport and quenching of chlorophyll fluorescence,
724 Biochim. Biophys. Acta BBA - Gen. Subj. 990 (1989) 87–92.
725 https://doi.org/10.1016/S0304-4165(89)80016-9.

726 [44] W.L. Webb, M. Newton, D. Starr, Carbon dioxide exchange of Alnus rubra,
727 Oecologia. 17 (1974) 281–291. https://doi.org/10.1007/BF00345747.

728 [45] R.K. Iler, Isolation and characterization of particle nuclei during the
729 polymerization of silicic acid to colloidal silica, J. Colloid Interface Sci. 75 (1980) 138–
730 148. https://doi.org/10.1016/0021-9797(80)90357-4.

731 [46] F.S. Sunlu, B. Buyukisik, T. Koray, U. Sunlu, Growth Kinetics of Cylindrotheca
732 closterium (Ehrenberg) Reimann and Lewin Isolated from Aegean Sea Coastal Water

733 (Izmir Bay/Türkiye), (2006). http://agris.fao.org/agris-
734 search/search.do?recordID=AV20120134053

735 [47] S. Sadati, M.K. Moradllo, M. Shekarchi, Long-term durability of onshore coated
736 concrete —chloride ion and carbonation effects, Front. Struct. Civ. Eng. 10 (2016) 150–
737 161. https://doi.org/10.1007/s11709-016-0341-2.

738 [48] P.M. Dove, The dissolution kinetics of quartz in sodium chloride solutions at 25
739 degrees to 300 degrees C, Am. J. Sci. 294 (1994) 665–712.
740 https://doi.org/10.2475/ajs.294.6.665.

741 [49] R. Ragoug, O.O. Metalssi, F. Barberon, J.-M. Torrenti, N. Roussel, L. Divet, J.-
742 B. d'Espinose de Lacaillerie, Durability of cement pastes exposed to external sulfate
743 attack and leaching: Physical and chemical aspects, Cem. Concr. Res. 116 (2019) 134–
744 145. https://doi.org/10.1016/j.cemconres.2018.11.006.

745 [50] L.S. Dent Glasser, N. Kataoka, The Chemistry of A.A.R, Cement Concrete. Res
746 11(1) (1981) 1–9

747 [51] S. Sjöberg, Y. Hägglund, A. Nordin, N. Ingri, Equilibrium and structural studies
748 of silicon(iv) and aluminium(iii) in aqueous solution. V. Acidity constants of silicic acid
749 and the ionic product of water in the medium range 0.05–2.0 M Na(CI) at 25°C, Mar.
750 Chem. 13 (1983) 35–44. https://doi.org/10.1016/0304-4203(83)90047-6.

751 [52] S. Sjöberg, A. Nordin, N. Ingri, Equilibrium and structural studies of silicon(IV)
752 and aluminium(III) in aqueous solution. II. Formation constants for the monosilicate ions
753 SiO(OH)3− and SiO2(OH)22−. A precision study at 25°C in a simplified seawater
754 medium, Mar. Chem. 10 (1981) 521–532. https://doi.org/10.1016/0304-4203(81)90005-
755 0.

[53] Y. Del Amo, M.A. Brzezinski, The Chemical Form of Dissolved Si Taken up by Marine Diatoms, J. Phycol. 35 (1999) 1162–1170. https://doi.org/10.1046/j.1529-8817.1999.3561162.x.

[54] A. Seidel, M. Löbbus, W. Vogelsberger, J. Sonnefeld, The kinetics of dissolution of silica 'Monospher' into water at different concentrations of background electrolyte, Solid State Ion. 101–103 (1997) 713–719. https://doi.org/10.1016/S0167-2738(97)00289-0.

[55] P.G. Falkowski, J.A. Raven, Aquatic Photosynthesis: (Second Edition), STU-Student edition, Princeton University Press, 2007. https://www.jstor.org/stable/j.ctt4cgbxs (accessed December 11, 2020).

[56] P. Claquin, A. Leynaert, A. Sferratore, J. Garnier, O. Ragueneau, Physiological Ecology of Diatoms Along the River–Sea Continuum, in: Silicon Cycle Hum. Perturbations Impacts Aquat. Syst., SCOPE 66, 2006: pp. 121–138.

[57] S. Capellacci, C. Battocchi, S. Casabianca, M. Giovine, G. Bavestrello, A. Penna, Bioavailability of different chemical forms of dissolved silica can affect marine diatom growth, Mar. Ecol. 34 (2013) 103–111. https://doi.org/10.1111/j.1439-0485.2012.00529.x.

[58] K. Hinga, Effects of pH on coastal marine phytoplankton, Mar. Ecol.-Prog. Ser. - MAR ECOL-PROGR SER. 238 (2002) 281–300. https://doi.org/10.3354/meps238281.

[59] D. Thornton, Diatom aggregation in the sea: mechanisms and ecological implications, Eur. J. Phycol. 37 (2002) 149–161. https://doi.org/10.1017/S0967026202003657.

778 [60] B. Moriceau, M. Garvey, U. Passow, O. Ragueneau, Evidence for reduced
779 biogenic silica dissolution rates in diatom aggregates, Mar. Ecol. Prog. Ser. 333 (2007)
780 129–142. https://doi.org/10.3354/meps333129.

781 [61] B. Moriceau, G.G. Laruelle, U. Passow, P. Van Cappellen, O. Ragueneau,
782 Biogenic silica dissolution in diatom aggregates: Insights from reactive transport
783 modelling, Mar. Ecol. Prog. Ser. 517 (2014) 35–49. https://doi.org/10.3354/meps11028.

784 [62] J.-P. Parkhill, G. Maillet, J.J. Cullen, Fluorescence-Based Maximal Quantum
785 Yield for Psii as a Diagnostic of Nutrient Stress, J. Phycol. 37 (2001) 517–529.
786 https://doi.org/10.1046/j.1529-8817.2001.037004517.x.

787 [63] C. Napoléon, V. Raimbault, P. Claquin, Influence of Nutrient Stress on the
788 Relationships between PAM Measurements and Carbon Incorporation in Four
789 Phytoplankton Species, PLOS ONE. 8 (2013) e66423.
790 https://doi.org/10.1371/journal.pone.0066423.

791 [64] A. Jungandreas, H. Wagner, C. Wilhelm, Simultaneous Measurement of the
792 Silicon Content and Physiological Parameters by FTIR Spectroscopy in Diatoms with
793 Siliceous Cell Walls, Plant Cell Physiol. 53 (2012) 2153–2162.
794 https://doi.org/10.1093/pcp/pcs144.

795 [65] E. Paasche, Silicon and the ecology of marine plankton diatoms. I. Thalassiosira
796 pseudonana (Cyclotella nana) grown in a chemostat with silicate as limiting nutrient, Mar.
797 Biol. 19 (1973) 117–126. https://doi.org/10.1007/BF00353582.

798 [66] N. Javaheri, R. Dries, J. Kaandorp, Understanding the Sub-Cellular Dynamics of
799 Silicon Transportation and Synthesis in Diatoms Using Population-Level Data and

800 Computational Optimization, PLoS Comput. Biol. 10 (2014) e1003687.
801 https://doi.org/10.1371/journal.pcbi.1003687.

802 [67] M. Hildebrand, Silicic Acid Transport and Its Control During Cell Wall
803 Silicification in Diatoms, in: Biominer. Prog. Biol. Mol. Biol. Appl., 2005: pp. 159–176.
804 https://doi.org/10.1002/3527604138.ch10.

805 [68] H.M. McNair, M.A. Brzezinski, J.W. Krause, Diatom populations in an upwelling
806 environment decrease silica content to avoid growth limitation, Environ. Microbiol. 20
807 (2018) 4184–4193. https://doi.org/10.1111/1462-2920.14431.

808 [69] S. Bonato, Étude de la variabilité spatiale et temporelle des communautés
809 phytoplanctoniques en Manche Orientale - Utilisation de la cytométrie en flux de
810 scanning, phdthesis, Université du Littoral Côte d'Opale, 2015. https://tel.archives-
811 ouvertes.fr/tel-01337264 (accessed August 31, 2021).

812 [70] M. Pahlow, U. Riebesell, D.A. Wolf-Gladrow, Impact of cell shape and chain
813 formation on nutrient acquisition by marine diatoms, Limnol. Oceanogr. 42 (1997) 1660–
814 1672. https://doi.org/10.4319/lo.1997.42.8.1660.

815 [71] K. Thamatrakoln, M. Hildebrand, Silicon Uptake in Diatoms Revisited: A Model
816 for Saturable and Nonsaturable Uptake Kinetics and the Role of Silicon Transporters,
817 Plant Physiol. 146 (2008) 1397–1407. https://doi.org/10.1104/pp.107.107094.

818 [72] A. Leynaert, S.N. Longphuirt, P. Claquin, L. Chauvaud, O. Ragueneau, No limit?
819 The multiphasic uptake of silicic acid by benthic diatoms, Limnol. Oceanogr. 54 (2009)
820 571–576. https://doi.org/10.4319/lo.2009.54.2.0571.

821 [73] S. Vanucci, L. Pezzolesi, R. Pistocchi, P. Ciminiello, C. Dell'Aversano, E.D.
822 Iacovo, E. Fattorusso, L. Tartaglione, F. Guerrini, Nitrogen and phosphorus limitation
823 effects on cell growth, biovolume, and toxin production in Ostreopsis cf. ovata, Harmful
824 Algae. 15 (2012) 78–90. https://doi.org/10.1016/j.hal.2011.12.003.

825